J Mater Sci (2007) 42:5680–5685
DOI 10.1007/s10853-006-0538-1

The crystallographic orientation relationship between Al_2O_3 and $MgAl_2O_4$ in the composite material Al_2O_3/Al–Mg–Si alloy

Susumu Ikeno · Kenji Matsuda · Toshimasa Matsuki · Toshiaki Suzuki · Noriaki Endo · Tokimasa Kawabata · Yasuhiro Uetani

Received: 13 December 2005 / Accepted: 6 June 2006 / Published online: 14 April 2007

Abstract The formation mechanism of spinels on Al_2O_3 particles in the Al_2O_3/Al–1.0 mass% Mg_2Si alloy composite material has been investigated by transmission electron microscopy (TEM) in order to determine the crystallographic orientation relationship. A thin sample of the Al_2O_3/Al–Mg–Si alloy composite material was obtained by the FIB method, and the orientation relationship between Al_2O_3 and $MgAl_2O_4$, which was formed on the surface of Al_2O_3 particles, was discovered by the TEM technique as follows:

$$\{111\}_{MgAl_2O_4}//\{0001\}_{Al_2O_3}$$

$$[2\bar{1}\bar{1}]_{MgAl_2O_4}//[2\bar{1}\bar{1}0]_{Al_2O_3}, [1\bar{1}0]_{MgAl_2O_4}//[1\bar{1}00]_{Al_2O_3}$$

At the interface between the Al_2O_3 and the matrix the $MgAl_2O_4$ (spinel) crystals had facets of {111} planes. Spinels were not grown as thin films, but as particles consisting of {111} planes. They grow towards both the matrix and the Al_2O_3 particles.

S. Ikeno · K. Matsuda (✉) · T. Kawabata
Faculty of Engineering, University of Toyama, 3190 Gofuku, Toyama 930-8555, Japan
e-mail: matsuda@eng.u-toyama.ac.jp

T. Matsuki
Graduate School, University of Toyama, 3190 Gofuku, Toyama 930-8555, Japan

Present Address:
T. Matsuki
Aishin Keikinzoku, Co. Ltd., Shin-minato, Toyama 934-8588, Japan

T. Suzuki · N. Endo
JEOL Ltd., 1-2, Musashino, 3-chome, Akishima, Tokyo 196-8558, Japan

Y. Uetani
Research Institute of Technology, Toyama Prefectural University, 5180, Kosugi, Imizu, Toyama 939-0398, Japan

Introduction

Al-alloy matrix/ceramic particles composite materials are being developed in order to profit from their high heat and wear resistance. Several types of composite materials with age-hardenable Al alloys as the matrix have been considered in our recent studies oriented towards their hardening behavior and precipitation process. Examples include systems such as Al_2O_3/Al–Mg–Si, Al_2O_3/Al–Cu–Mg, SiC/Al–Mg–Si, SiC/Al–Cu–Mg, etc. [1–5]. Table 1 shows their age-hardening behavior and precipitation processes. Composite materials containing Al_2O_3 particles show a lower hardness and different precipitation sequence. Owing to the formation of $MgAl_2O_4$ (spinel) crystals at the interface between ceramic particles and the matrix, the Mg content in the matrix is reduced and the precipitation sequences modify to phases not containing Mg [1, 2]. Because of this mechanism, the Al_2O_3/Al–1.0 mass%Mg_2Si composite showed the same precipitation sequence as the Al–0.6 mass%Mg_2Si–0.2 mass%Si alloy. Even the Al_2O_3/Al–Cu–Mg alloy composite material exhibited a precipitation process similar to that in an Al–Cu alloy. It is well known that the $MgAl_2O_4$ (spinel) is also formed in other Al alloys, for example in the Al_2O_3/Al–Mg and Al_2O_3/Al–Si–Mg alloy composite materials according to following schemes [6–9]:

Table 1 Summary of hardening behavior and precipitation process of Al-alloy matrix / ceramic particles composite materials in our recent studies [1–5]

	Al–1.0 mass% Mg_2Si alloy			Al–4 mass% Cu–2 mass% Mg alloy		
	SiC	TiC	Al_2O_3	SiC	TiC	Al_2O_3
Peak hardness at 473 K	+	–	–	+	+	–
Age-hardenability* at 473 K	–	–	–	+	+	–
Precipitation process	changed	not changed	changed	changed	not changed	changed

(+) and (–) indicate positive or negative changes for each property.

*The age-hardenability is the difference between hardness values of peak aged and as-quenched samples.

$$Mg\ (l) + 2Al\ (l) + 2O_2 \rightarrow MgAl_2O_4\ (s) \quad (1)$$

$$MgO\ (s) + Al_2O_3\ (s) \rightarrow MgAl_2O_4\ (s) \quad (2)$$

$$Mg\ (l) + \frac{4}{3}Al_2O_3\ (s) \rightarrow MgAl_2O_4\ (s) + \frac{2}{3}Al\ (l) \quad (3)$$

Several reports exist about the chemical reaction responsible for spinel formation [6–9], though its crystallography between Al_2O_3 and spinel in Al-based composite materials has not yet been clarified. In this study, the formation mechanism of spinels on Al_2O_3 particles in the Al_2O_3/Al–1.0 mass%Mg_2Si alloy composite material has been investigated by transmission electron microscopy (TEM) in order to determine the crystallographic orientation relationship.

Experimental

The Al–1.0 mass%Mg_2Si matrix alloy was prepared by melting from 99.99 mass% pure aluminum and 99.9 mass% pure silicon and magnesium ingots, and the molten alloy was cast into an iron mold. α-Al_2O_3 particles used for reinforcement were provided by Sumitomo Chemicals Co. Ltd. Their mean diameter was 1.5 μm, the purity was at least 99.9%, and impurities of Si, Fe and Na were below 11 ppm. Preparation of the composite material of 4 vol.% Al_2O_3/Al–1.0 mass%Mg_2Si alloy was performed as follows: the Al_2O_3 particles were poured into the bottom of a steel mold and then the molten metal was injected by a press machine through a small aperture. The mold was rapidly cooled by a water jacket from the bottom. Billets of 30 mm in diameter and 50 mm in length were hot-extruded into a bar of ϕ 10 mm, and then cut into thin discs. These discs were solution heat-treated at 848 K for 3.6 ks, quenched in chilled water, and then aged at 473 K for 24 ks [1]. TEM samples were generally prepared by the electrolytic polishing technique. FIB was also used to obtain TEM samples of a thickness of less than 200 nm. The TEM used was the Topcon EM002B at 200 kV, equipped with energy-dispersive X-ray spectroscopy (EDS), and the JEOL 4010T with the feature of generating elemental maps via an energy filter.

Results and discussion

Figure 1 shows TEM images of the composite material when the TEM sample was treated by the conventional electro-polishing technique. The large dark features correspond to the Al_2O_3 particles, and rod-shaped precipitates are also visible in the matrix. The distribution of precipitates is inhomogeneous, and this fact causes the peak hardness of the composite material reduced below that of the matrix alloy [1]. From the particle shown in the middle of Fig. 1, electron diffraction patterns (SADP) were attempted, but this particle was too thick to provide clear patterns. The electrolytic polishing method does not remove the Al_2O_3 material, although the Al alloy matrix is dissolved well. As it was too difficult to obtain clear

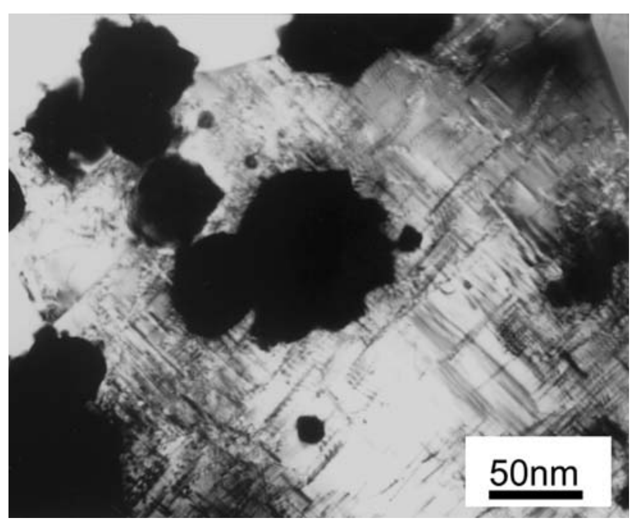

Fig. 1 The bright field TEM image of the composite material. The specimen was prepared by the conventional electro-polishing technique

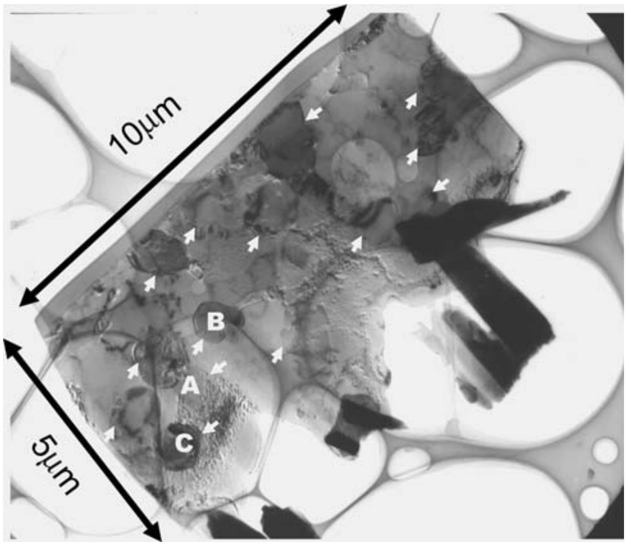

Fig. 2 The bright field TEM image of the composite material. The specimen was prepared by the FIB method and mounted on a carbon mesh

SADPs from the Al_2O_3 particles, as well as from the reaction products at the interface between the matrix and the particles, the FIB method was applied to preparation of sufficiently thin TEM samples. Figure 2 shows a TEM image of such a thin specimen made by the FIB method and mounted on a carbon mesh. While in Fig. 1 the ceramic particles appeared just as dark spots, here some details on them are reproduced. The aluminum matrix, however, is locally damaged in many places by the Ga ion beam.

Figure 3 presents TEM micrographs of the particle marked A in Fig. 2. White arrows point in both Fig 3(a) and (b) to identical features that were identified as spinel ($MgAl_2O_4$) crystals. An EDS analysis was performed for particles X and Y in Fig. 3(b). Particle X was of Al_2O_3 as it showed only O and Al peaks, but particle Y is the spinel, $MgAl_2O_4$, as elements O, Mg and Al were all detected here. The particles marked by the white arrows were both identified as spinels embedded in the Al_2O_3 particle marked X.

Figure 4 shows the corresponding SADPs, which again can be identified as those of $MgAl_2O_4$ and Al_2O_3, respectively. The mutual orientation relationship is obvious from these SADPs. The Al_2O_3 particle shows facets that are parallel to $[\bar{1}\bar{1}20]$ and $[2\bar{1}\bar{1}0]$ directions in the particle. $MgAl_2O_4$ also shows facets, which are here parallel to $[10\bar{1}]$ and $[0\bar{1}1]$ directions. Figure 5 is a schematic illustration of the relationship between the diffraction patterns of Al_2O_3 and the spinel in Fig. 4. $[111]_{MgAl_2O_4}$ is parallel to $[0001]_{Al_2O_3}$ and $[2\bar{1}\bar{1}]_{MgAl_2O_4}$ is parallel to $[2\bar{1}\bar{1}0]_{Al_2O_3}$. Furthermore, $[1\bar{1}0]_{MgAl_2O_4}$ direction is parallel to $[1\bar{1}00]_{Al_2O_3}$. In Fig. 6 another particle is represented, exhibiting the same orientation relationship as that in Fig. 4. In Fig. 2 this particle was marked B and the $[1\bar{1}00]_{Al_2O_3}$ direction was found parallel to $[1\bar{1}0]_{MgAl_2O_4}$ in this case.

Fig. 3 TEM pictures obtained from the particle marked A in Fig. 2: the bright field image (**a**), and the dark field image (**b**). EDS profiles obtained from particles marked in Fig. 3(**b**) as X (**c**), and Y (**d**)

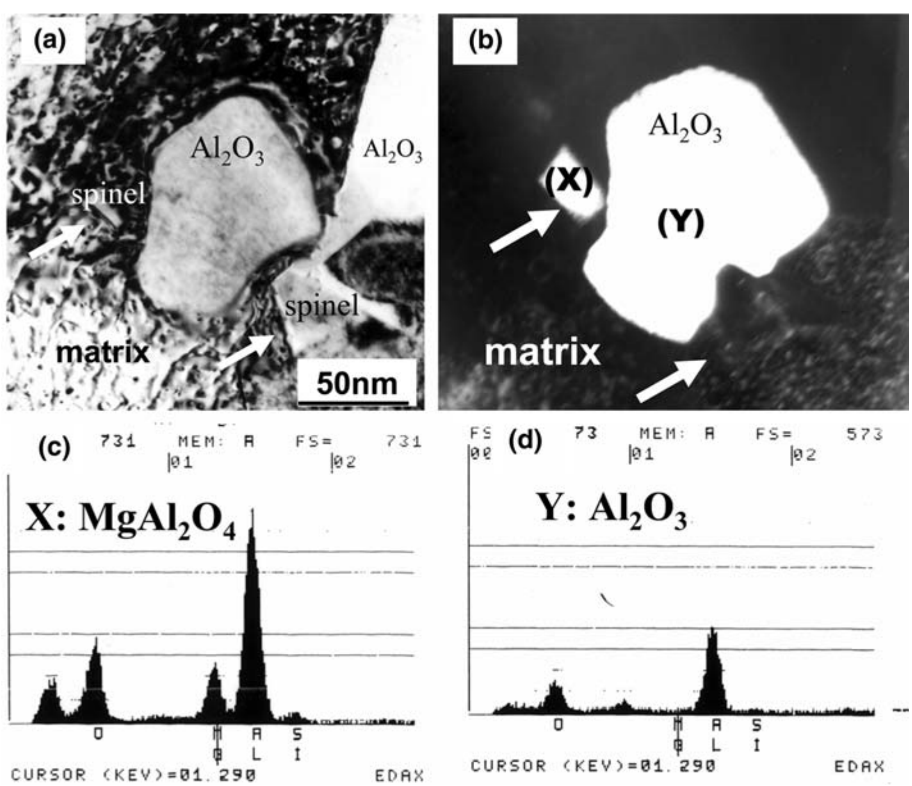

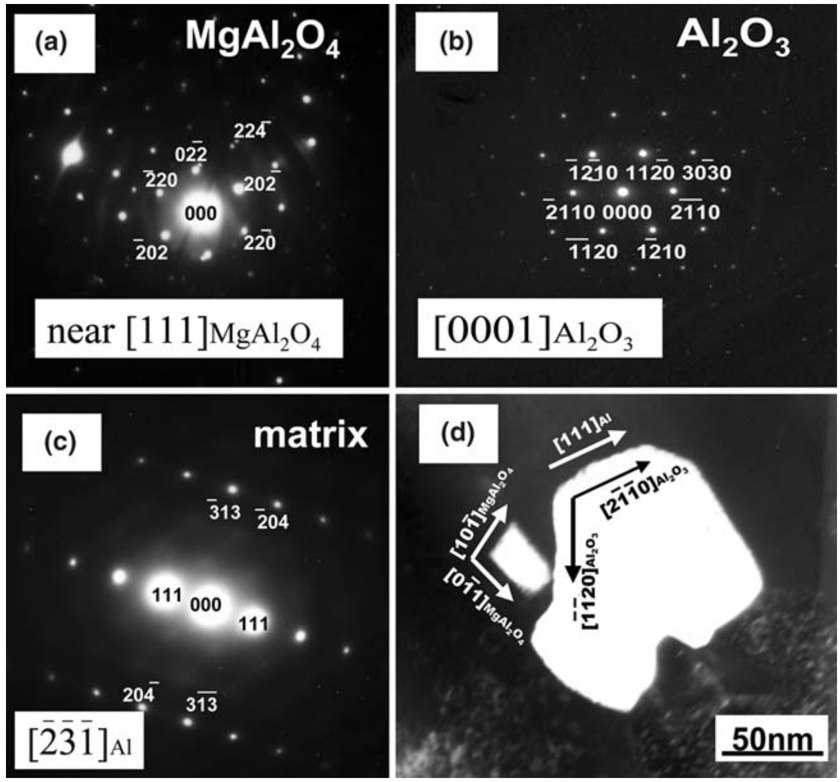

Fig. 4 SADPs obtained from particles marked in Fig. 3(**b**) as X (**a**), and Y (**b**), together with SADP of the matrix (**c**). Figure (**d**) shows the dark field image indexed according to SADPs in figs. (**a**)–(**c**)

Figure 7 summarizes the orientation relationships obtained. Basically, $[111]_{MgAl_2O_4}$ is parallel to $[0001]_{Al_2O_3}$, $[2\bar{1}\bar{1}0]_{Al_2O_3}$ is parallel to $[2\bar{1}\bar{1}]_{MgAl_2O_4}$, and $[1\bar{1}00]_{Al_2O_3}$ is parallel to $[1\bar{1}0]_{MgAl_2O_4}$. The results in Figs. 4 and 6 can be explained using this diagram. If the {111} plane of $MgAl_2O_4$ is parallel to {0001} plane of Al_2O_3, these relationships are straightforward. Altogether, the following orientation relationship can be proposed on the basis of the present work:

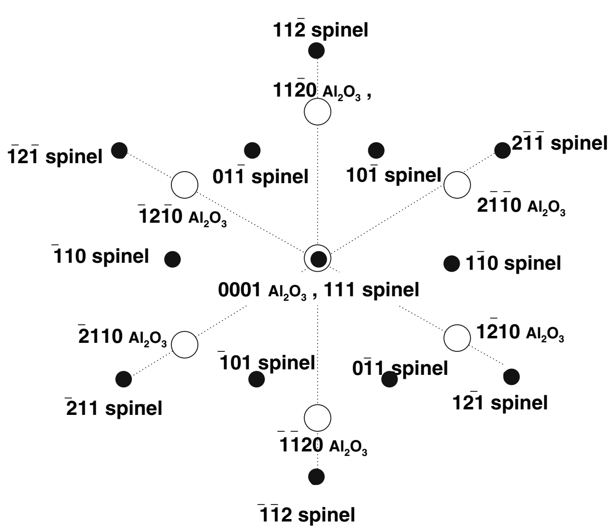

Fig. 5 Schematic illustration of the relationship between the diffraction patterns of Al_2O_3 and the spinel in Fig. 4

$$\{111\}_{MgAl_2O_4}//\{0001\}_{Al_2O_3}$$

$$[2\bar{1}\bar{1}]_{MgAl_2O_4}//[2\bar{1}\bar{1}0]_{Al_2O_3}, [1\bar{1}0]_{MgAl_2O_4}//[1\bar{1}00]_{Al_2O_3}$$

The first report of an identical orientation relationship between nickel aluminate spinel and alumina was published by Thirsk and Whitmore [10] and Li et al. examined $MgAl_2O_4$ formed at the interface between MgO and Al_2O_3 [11]. Those spinels were formed on {0001} plane of α-Al_2O_3. In our study, we found a similar relationship between the Al_2O_3 and $MgAl_2O_4$ structures to previous reports, however, no relationship between the Al-matrix and Al_2O_3 or $MgAl_2O_4$ particles was possible to establish. Carter and Schmalzried reported the orientation relationship between cobalt aluminate spinel and alumina, and they found that for a (0001) alumina substrate, the (111) plane of the spinel was slightly inclined to the basal plane of the α-Al_2O_3 [12]. In the present work, Fig. 4(a) was near [111] of spinel, not exactly at [111] of spinel, and the $[1\bar{1}00]_{Al_2O_3}$ diffraction pattern was slightly off the exact zone axis orientation in Fig. 6(b). These results possibly support the result of Carter and Schmalzried.

Figure 8 shows EFTEM pictures of the interface between the particle marked C in Fig. 2 and the matrix. In Fig. 8(b) two white arrows mark the interface in question—it is quite straight and apparently does not contain any reaction products. Figure 8(c) shows an elemental map of the Mg–K edge obtained from the same area, which

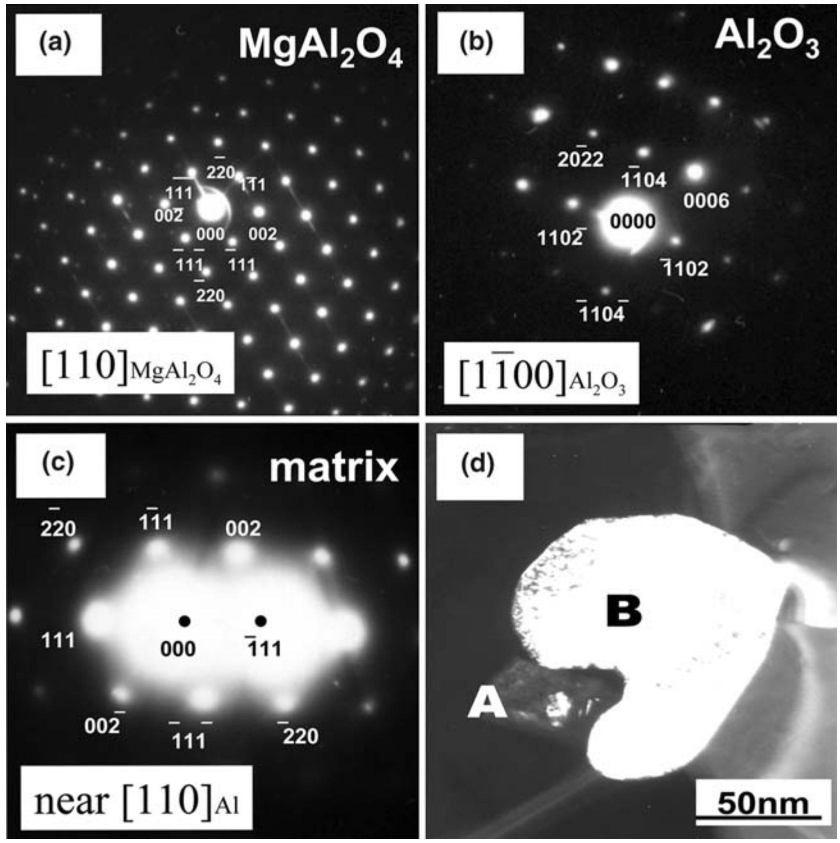

Fig. 6 SADPs obtained from the area marked in Fig. 2 as B: SADPs from particles marked in the dark field image (**d**) of this area as A (**a**) and B in (**b**), together with SADP of the matrix (**c**)

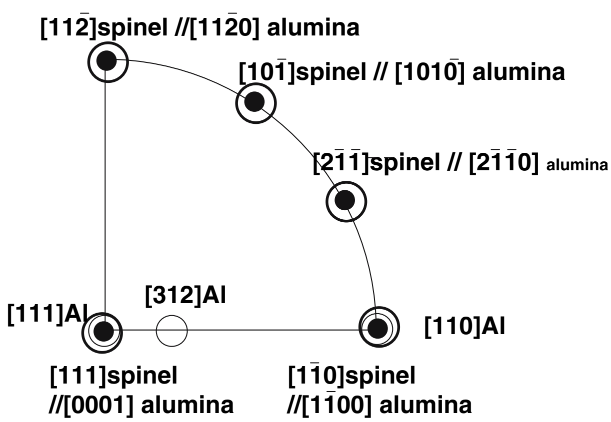

Fig. 7 Summary of orientation relationships between $MgAl_2O_4$, Al_2O_3 and the Al-matrix

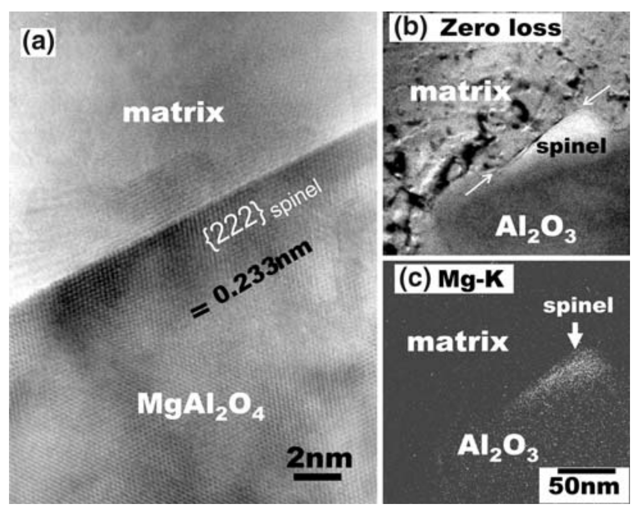

Fig. 8 EFTEM pictures of the interface between the particle marked in Fig. 2 as C, and the matrix: high resolution image (**a**), zero-loss image (**b**), and the Mg–K map obtained from the same area (**c**)

proves the presence of Mg, so this part of the particle is a spinel crystal, i.e. the reaction product itself. Figure 9 shows EFTEM pictures of another part of the same interface that is again straight, there is no $MgAl_2O_4$ here and the $\{2\bar{1}\bar{1}0\}$ plane of Al_2O_3 is nearly parallel to {111} plane of the matrix. Homogeneous distribution of oxygen is recognized in the O–K map in Fig. 9(c).

Rao and Jayaram [8] investigated Al_2O_3/Al–Mg alloy composite materials and reported the existence of MgO and $MgAl_2O_4$ as reacted products. In the present work, however, no MgO has been revealed and the mechanism of formation of $MgAl_2O_4$ in this composite material results as follows. First of all, a small melted region on an Al_2O_3 particle directly transforms into $MgAl_2O_4$ so a nucleus of this composition is created at the interface

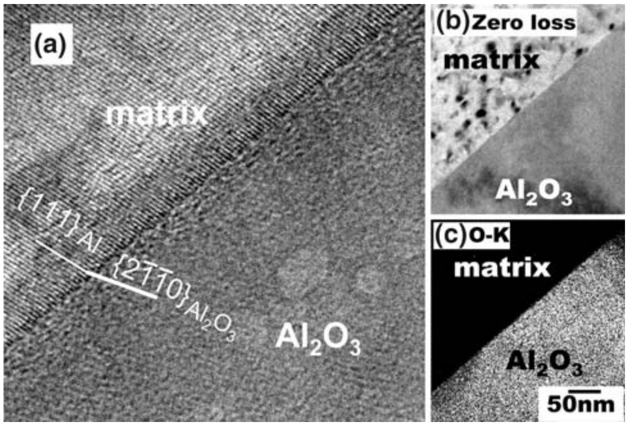

Fig. 9 EFTEM pictures of another part of the interface between the particle marked in Fig. 2 as C, and the matrix: high resolution image (**a**), zero-loss image (**b**), and the O–K map obtained from the same area (**c**)

to the matrix. Then this nucleus keeps growing to a particle having facets securing minimum interfacial energy. In this process the Mg atoms come from the matrix while the oxide is taken from the ceramic particle, so that the spinel grows in both directions from the original interface. The reactions could take place during the process of forming the billet and/or extrusion. This model explains why in Figs. 2 and 3 the $MgAl_2O_4$ particles are embedded in the Al_2O_3 particles.

Conclusions

A thin sample of the Al_2O_3/Al–Mg–Si alloy composite material was obtained by the FIB method, and the orientation relationship between Al_2O_3 and $MgAl_2O_4$, which was formed on the surface of Al_2O_3 particles, was discovered by the TEM technique as follows:

$$\{111\}_{MgAl_2O_4}//\{0001\}_{Al_2O_3}$$

$$[2\bar{1}\bar{1}]_{MgAl_2O_4}//[2\bar{1}\bar{1}0]_{Al_2O_3},\ [1\bar{1}0]_{MgAl_2O_4}//[1\bar{1}00]_{Al_2O_3}$$

At the interface between the Al_2O_3 and the matrix the $MgAl_2O_4$ (spinel) crystals had facets of {111} planes. Spinels were not grown as thin films, but as particles consisting of {111} planes. They grow towards both the matrix and the Al_2O_3 particles.

Acknowledgement Authors thank to Mr. Hiroaki Matsui, formerly Master's Student, Graduate School, Toyama University, is with Aishin-Keikinzoku Co. Ltd. (Toyama, 934-8588, Japan) for his experimental support.

References

1. Ikeno S, Araki M, Matsuda K, Shinagawa F, Uetani Y (1999) J Japan Inst Light Metal 49:244
2. Ikeno S, Matusda K, Teraki T, Terayama K, Rengakuji S, Shinagawa F, Uetani Y (1997) J Japan Inst Light Metal 47:421
3. Ikeno S, Matsuda K, Rengakuji S, Uetani Y (2001) J Mater Sci 36:1921
4. Ikeno S, Matsui H, Matsuda K, Uetani Y (2000) Mater Sci Forum 331–337:1193
5. Ikeno S, Furuta K, Teraki T, Matsuda K, Anada H, Uetani Y (1996) J Japan Inst Light Metals 46:9
6. Lee KB, Kim YS, Kwon H (1998) Met Mater Trans A 29A:3087
7. Lu P, Loehman RE, Ewsuk KG, Fahrenholtz WG (1999) Acta Mater 47:3099
8. Rao BS, Jayaram V (2001) Acta Mater 49:2373
9. Daoud A, Reif W (2002) J Mater Process Tech 123:313
10. Thirsk HR, Whitmore EJ (1940) Trans Faraday Soc 36:565
11. Li DX, Pirouz P, Heuer AH (1992) Phil Mag A 65:403
12. Carter CB, Schmalzried H (1985) Phil Mag A 52:207